Characterization and Localization of Two Ion-binding Sites within the Pore of Cardiac L-Type Calcium Channels

ROBERT L. ROSENBERG and XIAO-HUA CHEN

From the Departments of Pharmacology and Physiology, University of North Carolina at Chapel Hill, Chapel Hill, North Carolina 27599

ABSTRACT L-type Ca channels from porcine cardiac sarcolemma were incorporated into planar lipid bilayers. We characterized interactions of permeant and blocking ions with the channel's pore by (*a*) studying the current–voltage relationships for Ca^{2+} and Na^+ when equal concentrations of the ions were present in both internal and external solutions, (*b*) testing the dose-dependent block of Ba^{2+} currents through the channels by internally applied cadmium, and (*c*) examining the dose and voltage dependence of the block of Na^+ currents through the channels by internally and externally applied Ca^{2+}. We found that the *I-V* relationship for Na^+ appears symmetrical through the origin when equal concentrations of Na^+ are present on both sides of the channel (γ = 90 pS in 200 mM NaCl). The conductance for outward Ca^{2+} currents with 100 mM Ca^{2+} on both sides of the channel is ~8 pS, a value identical to that observed for inward currents when 100 mM Ca^{2+} was present outside only. This provides evidence that ions pass through the channel equally well regardless of the direction of net flux. In addition, we find that internal Cd^{2+} is as effective as external Cd^{2+} in blocking Ba^{2+} currents through the channels, again suggesting identical interactions of ions with each end of the pore. Finally, we find that micromolar Ca^{2+}, either in the internal or in the external solution, blocks Na^+ currents through the channels. The affinity for internally applied Ca^{2+} appears the same as that for externally applied Ca^{2+}. The voltage dependence of the Ca^{2+}-block suggests that the sites to which Ca^{2+} binds are located ~15% and ~85% of the electric field into the pore. Taken together, these data provide direct experimental evidence for the existence of at least two ion binding sites with high affinity for Ca^{2+}, and support the idea that the sites are symmetrically located within the electric field across L-type Ca channels.

INTRODUCTION

Dihydropyridine-sensitive L-type Ca channels support a rapid influx of Ca^{2+}, with a single-channel conductance of ~8 pS in 100 mM Ca^{2+} (Hess, Lansman, and Tsien, 1986). These channels are highly selective for Ca^{2+} over monovalent cations, with $P_{Ca}/P_{Na} > 1{,}000$ when measured as a reversal potential under bi-ionic conditions (Lee

Address reprint requests to Dr. Robert L. Rosenberg, Department of Pharmacology, CB #7365, University of North Carolina at Chapel Hill, Chapel Hill, NC 27599-7365.

J. GEN. PHYSIOL. © The Rockefeller University Press · 0022-1295/91/06/1207/19 $2.00
Volume 97 June 1991 1207–1225

and Tsien, 1984; Campbell, Giles, Hume, Noble, and Shibata, 1988*a*). However, Ca channels can carry large monovalent currents (Kostyuk, Mironov, and Shuba, 1983; Almers, McCleskey, and Palade, 1984; Fukushima and Hagiwara, 1985; Coronado and Affolter, 1986; Hess et al., 1986; Rosenberg, Hess, Reeves, Smilowitz, and Tsien, 1986; Hadley and Hume, 1987); in the absence of extracellular Ca^{2+}, the conductance of L-type Ca channels for Na^+ is 90 pS, more than an order of magnitude larger than that for Ca^{2+} (Hess et al., 1986).

Two classes of models have been proposed to account for these and other features of ion permeation through Ca channels: (1) Ca^{2+} binds to sites on the external surface of the channel, and occupancy of those sites by Ca^{2+} causes Ca^{2+}-selectivity by allosteric control of the selectivity mechanism (Kostyuk et al., 1983; Kostyuk and Mironov, 1986); and (2) Ca^{2+} binds with high affinity to more than one site within the pore (Almers and McCleskey, 1984; Hess and Tsien, 1984). Occupancy of at least one intrapore site by Ca^{2+} prevents the permeation of other ions (securing Ca^{2+}-selectivity) and occupancy of more than one site by Ca^{2+} provides for the high flux rate because ion–ion repulsion hastens dissociation of Ca^{2+} from the high-affinity sites (for review see Tsien, Hess, McCleskey, and Rosenberg, 1987).

The first class of models is inconsistent with an accumulating mass of evidence. The block of unitary monovalent currents by Ca^{2+} and other divalent ions is voltage dependent, suggesting that the Ca^{2+}-binding site is within the transmembrane electric field, probably within the pore (Fukushima and Hagiwara, 1985; Lansman, Hess, and Tsien, 1986; Lansman, 1990). The large conductance for monovalent ions is not due to a global change in protein conformation arising from a lack of external Ca^{2+}, because even in the presence of 100 mM external Ca^{2+} the channels can carry large outward monovalent currents when the membrane is depolarized beyond the reversal potential (Rosenberg et al., 1986; Rosenberg, Hess, and Tsien, 1988). Increasing the concentration of Ba^{2+} increases the off-rate in Cd^{2+}- and Mg^{2+}-block, indicating interactions between permeant and blocking ions (Lansman et al., 1986).

The second class of models is appealing because of their simplicity and independence from allostery, although direct evidence supporting them is not overwhelming. In addition to the support mentioned above, these models are strengthened by the observation that when current amplitude is plotted versus the concentration of permeant ion, the data deviate significantly from the Langmuir isotherm predicted by a single-site model (Ma and Coronado, 1987; Yue and Marban, 1990). An important test that favors multi-ion occupancy is the "anomalous mole-fraction effect" (AMFE), where the current in the presence of mixtures of Ca^{2+} and Ba^{2+} is smaller than the current measured in the presence of either Ca^{2+} or Ba^{2+} alone (Hess and Tsien, 1984; Byerly, Chase, and Stimers, 1985; McDonald, Cavalie, Trautwein, and Pelzer, 1986; Friel and Tsien, 1989). However, single-channel currents through L-type Ca channels in intact cardiac myocytes do not demonstrate the AMFE (Yue and Marban, 1990; c.f. Friel and Tsien, 1989), and therefore these experiments do not provide unequivocal support for the multi-ion models.

Most of the Ca^{2+}-block experiments that provide the strongest support for the multi-ion models were performed with intact cells where only external Ca^{2+} could be applied. Block of unitary Na^+ currents by internal Ca^{2+} was shown in inside-out patches from heart cells (Hess, Prod'hom, and Pietrobon, 1989), but the experiments

were limited because of the rapid disappearance of L-type Ca channels from excised patches. However, L-type Ca channels from cardiac sarcolemma can be recorded for several minutes in planar lipid bilayers where there is access to the intracellular compartment (Rosenberg et al., 1986, 1988; Ehrlich, Schen, Garcia, and Kaczorowski, 1986). Thus, we set out to explore the interactions of monovalent and divalent cations with L-type Ca channels, especially from the internal solution, to determine the number and character of ion-binding sites within the pore.

A preliminary report of some of these results has appeared (Rosenberg, Chen, and Koplas, 1990).

METHODS

Preparation of Cardiac Sarcolemmal Vesicles

Hearts from young pigs were obtained from a local slaughterhouse, and sarcolemmal membrane fragments were prepared from left ventricular muscle as previously described (Rosenberg et al., 1988).

Planar Lipid Bilayers

Planar lipid bilayers were formed from decane solutions of 1-palmitoyl-2-oleoyl phosphatidylethanolamine (15 mg/ml) and 1-palmitoyl-2-oleoyl phosphatidylserine (5 mg/ml) across a 200-μm-diam hole in a polyvinyldifluoride partition. This mixture of synthetic lipids produced bilayers with greater stability than those from natural lipids used previously (Rosenberg et al., 1986, 1988), without affecting Ca channel gating and permeation properties. Lipids were obtained from Avanti Polar Lipids, Inc. (Pelham, AL) and were used without further purification.

At the time of bilayer formation, aqueous solutions contained 50 mM NaCl and 10 mM HEPES-NaOH, pH 7.0. The dihydropyridine agonist (+)-202-791 (Sandoz AG, Basel, Switzerland), in a stock solution of 5 mM in ethanol, was added to both chambers to a final concentration of 1 μM. To record Ca^{2+} or Ba^{2+} currents, divalent ions were added to the *cis* chamber from a 1 M stock solution. To record Na^+ currents, HEDTA was added to both chambers to a final concentration of 1 mM from a 100 mM stock solution, lowering free Ca^{2+} concentration to below 10 nM, and 150 mM NaCl (from a 3 M stock solution) was added to the *cis* chamber, providing the osmotic gradient that promotes vesicle fusion with bilayers (Cohen, 1986) and shifting E_{Na} to +35 mV and E_{Cl} to −35 mV. In all experiments, sarcolemmal vesicles were added to the *cis* chamber (~50 μg protein/ml final concentration).

Voltage clamp of the bilayers, recording of the currents, and analog and digital leak and capacitance compensation were performed as previously described (Rosenberg et al., 1988) except that an 80386-based computer running AxoBasic (Axon Instruments, Inc., Foster City, CA) was used. Voltages were defined as *trans* minus *cis*, and currents from *cis* to *trans* are shown as inward (negative) transitions as described previously (Rosenberg et al., 1988). Thus, the *trans* chamber represents the cellular interior, consistent with the conventional incorporation of outside-out vesicles. Bilayers were held at −60 to −80 mV for 5.2 s between 800-ms test pulses to 0 mV. Any channels that might have become incorporated into the bilayers with the opposite orientation would experience a large positive holding potential, and would probably be in the inactivated state (McDonald et al., 1986; Rosenberg et al., 1988). Even if inactivation at positive potentials was incomplete (Campbell, Giles, Hume, and Shibata, 1988*b*), the open probability of a channel with the reverse orientation would be much smaller than for those with the normal orientation. In addition, if inactivation of channels with reverse orientation was incomplete,

then robust activity at the holding potential would be expected. The very high levels of activity in most recordings, especially early in each experiment before "rundown" occurred, and the lack of activity at the negative holding potentials, provide evidence that the channels recorded had the expected orientation. Occasional experiments using a positive holding potential to test for the presence of channels with the reverse orientation were always negative ($n \approx 25$).

Channel activity appeared spontaneously, usually within 5 min, as inward current transitions of 0.4, 1.3, or 2.0 pA for Ca^{2+}, Ba^{2+}, or Na^+, respectively. Na^+ currents were also measured at other test potentials (usually −20 mV) to verify cation selectivity and conductance. Currents were filtered (8-pole Bessel lowpass; corner frequency 200 Hz), digitized at 1,000 Hz, and stored in computer memory for later analysis. Because of the large capacitance associated with the large bilayer area, the noise of these recordings was greater than in patch-clamp experiments; a fit of the Gaussian distribution to an amplitude histogram from a "bare" bilayer yielded a σ of 0.13 pA. Thus, the minimum current amplitude that could be resolved from the noise was ~0.26 pA (2σ).

Additions of NaCl, $CaCl_2$, or $CdCl_2$, as required for each experiment, were made from appropriate stock solutions. The concentration of free Ca^{2+} in solutions of Ca^{2+} and HEDTA was calculated using Eqcal88 (Biosoft, Milltown, NJ) with published stability constants for HEDTA (Martell and Smith, 1974).

Data Analysis

Leak-subtracted current recordings of Ca^{2+}-blocked Na^+ currents were analyzed as follows. Records of 1,024 points were processed by a cubic spline routine (Colquhoun and Sigworth, 1983), increasing the number of points to 5,120. The splined data set was then converted to an analog signal, filtered at 30 Hz, and rerecorded (0.2 ms/point sample rate). This refiltering routine was required to increase the time constant of the equivalent first-order filter (τ) so that the products of the unblocking rate (α) and the blocking rate (β) with the time constant τ, $\alpha\tau$ and $\beta\tau$, were greater than 2 (Yellen, 1984). At Ca^{2+} concentrations of ~1 μM, β was expected to be ~500 s^{-1} (Lansman et al., 1986); since $\tau = 0.228/f_c$ (where f_c is the corner frequency of an 8-pole Bessel lowpass filter), $\beta\tau > 2$ suggests that $f_c < 57$ s^{-1}.

The processed records were then used to form amplitude histograms. Periods of unambiguous channel openings with durations greater than 5 ms were selected for analysis. Channel closings of greater than 2 ms were excluded. This selection process would allow brief closing events to contaminate the selected periods, but the contribution of such rapid closing is expected to be minor because of the paucity of such events compared with the extent of block by Ca^{2+}.

Histograms of the blocked channel openings were fitted with the beta distribution (see Results) convolved with the Gaussian distribution that describes the closed-channel noise. The fit of the data was done by eye (Yellen, 1984).

RESULTS

Current–Voltage Relationships with Equal Concentrations of Permeant Ions on Both Sides of the Channel

Previous reports have demonstrated that L-type Ca channels show linear *I-V* relations with equal concentrations of Ba^{2+} (Rosenberg et al., 1986) and Na^+ (Hess et al., 1989) on both sides. An *I-V* relationship that is symmetrical through the origin is evidence of a functionally symmetric pore, because the currents on either side of the reversal potential are equal and opposite. We tested the *I-V* relation of L-type Ca channels in

planar lipid bilayers with equal concentrations of Na^+ and Ca^{2+}, to see if under our conditions the pore appeared functionally symmetrical to these two permeant ions.

Fig. 1 shows that L-type Ca channels in planar lipid bilayers also show a linear *I-V* relation for Na^+ permeation, confirming earlier reports (Hess et al., 1989). The conductance of the channels was 90 pS, in agreement with data from patches from heart cells (Hess et al., 1986, 1989).

The pH in this experiment was 7.5, compared with 8.5 in previous reports (Hess et al., 1989), and we had expected very rapid proton block of Na^+ current (Pietrobon and Hess, 1988; Pietrobon, Prod'hom, and Hess, 1989) to reduce the apparent

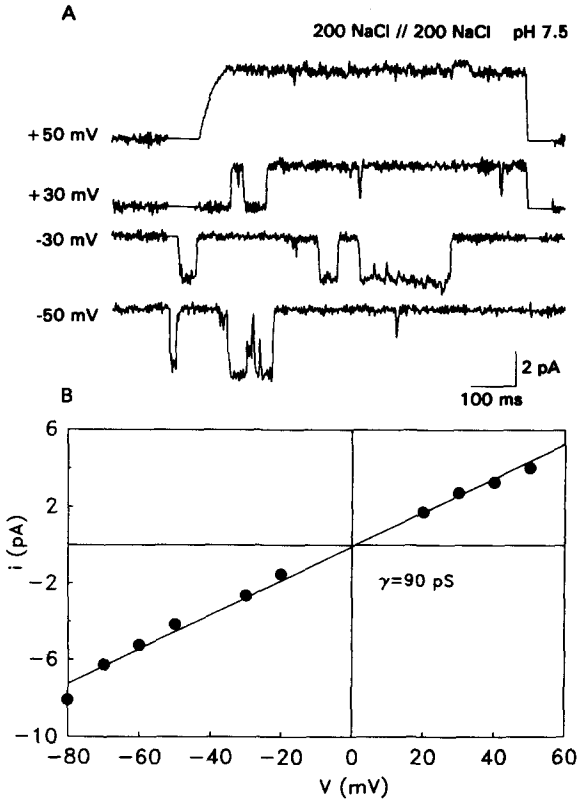

FIGURE 1. *I-V* relationship with 200 mM NaCl on both sides of the bilayer. Inward and outward currents were recorded with symmetrical solutions of 200 mM NaCl, 10 mM HEPES-NaOH (pH 7.5), and 1 mM HEDTA. Free Ca^{2+} was estimated to be <10 nM. (*A*) Current records obtained when the membrane was held at HP = −80 mV between pulses to the test potentials (TP) shown. The curved opening transition (*top record*) is an artifact of the recovery of the amplifier and analog-to-digital converter from saturation following the large depolarization. Current amplitudes were measured by eye with the aid of computer-drawn lines, and plotted (*B*) as a function of the test potential. The line represents the least-squares fit to the data, yielding a slope of 90 pS from −70 to +50 mV.

conductance in our experiments. Apparently, in 200 mM NaCl the extent of proton block at pH 7.5 was diminished compared with that in 150 mM NaCl (Pietrobon and Hess, 1988; Pietrobon et al., 1989). At pH 7.0 we observed a reduction of the conductance to ~75 pS, as expected (not shown). Increasing the pH above 7.5 was not feasible because of bilayer instability.

Fig. 2 shows an *I-V* relation when equal concentrations of Ca^{2+} were present on both sides of the channel. At positive voltages where openings could be recorded, the *I-V* relation showed an upward curvature. The slope conductance (0–100 mV) was ~8 pS, increasing to ~14 pS above 100 mV.

It was impossible to record inward currents in symmetrical Ca^{2+} because of the small amplitude at modest negative test potentials and the lack of channel activation at large negative test potentials. Tail current measurements after repolarization of the bilayer were not successful, because even in the presence of the dihydropyridine agonist the channels closed within the 30–40-ms period of amplifier and A/D converter saturation after the voltage jumps (c.f. Lansman et al., 1986). Thus, we

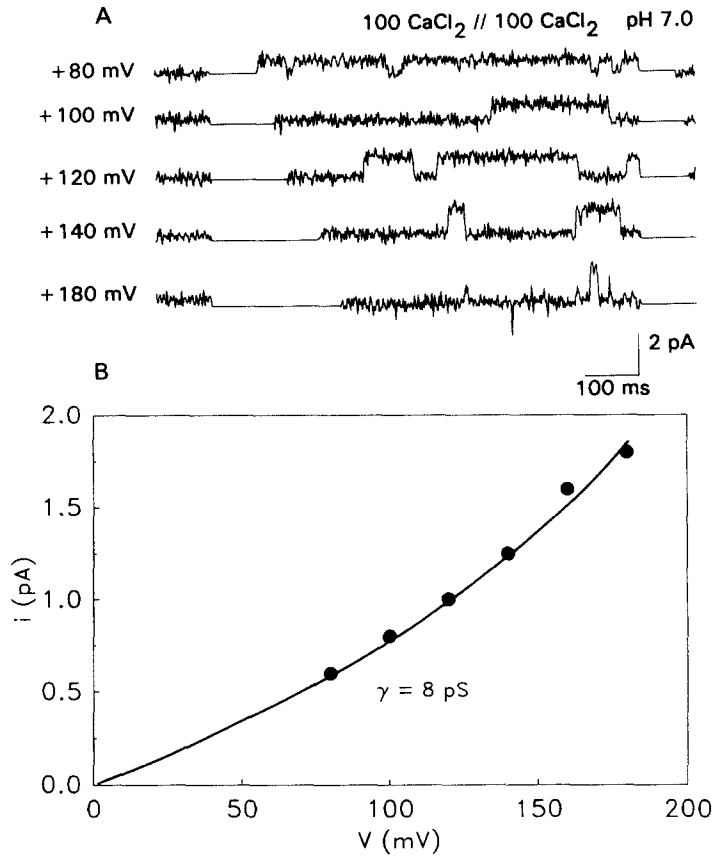

FIGURE 2. *I-V* relationship for L-type Ca channels in symmetrical 100 mM Ca^{2+}. Both solutions contained 100 mM $CaCl_2$, 50 mM NaCl, and 10 mM HEPES-NaOH (pH 7.0). (*A*) Currents were recorded at the test potential shown; HP = −80 mV. Current amplitudes were measured as in Fig. 1 and were plotted (*B*) vs. test potential. The curve was drawn by eye. The slope conductance was ~8 pS, increasing to ~14 pS at very large depolarizations.

could not determine if there was downward curvature of the *I-V* at large negative potentials similar to the upward curvature at large positive potentials.

Although the direct observation of symmetrical Ca^{2+} permeation is not possible under these conditions, we can draw comparisons with previous results. Under asymmetrical ionic conditions with 100 mM Ca^{2+} in the external solution only, the conductance for inward currents was 7–8 pS (Hess et al., 1986; Rosenberg et al.,

1988; Yue and Marban, 1990). Thus, the conductance for outward currents measured at modest depolarizations under conditions of symmetrical Ca^{2+} (~8 pS; Fig. 2) is equal to that of inward currents around 0 mV measured with Ca^{2+} present in the external solution only (7–8 pS; Hess et al., 1986; Rosenberg et al., 1988; Yue and Marban, 1990). By way of comparison, the conductance of L-type Ca channels around 0 mV with 100 mM Ba^{2+} present on the outside is ~25 pS (Hess et al., 1986; Rosenberg et al., 1986, 1988; Yue and Marban, 1990) and with 100 mM Ba^{2+} on both sides of the channel the *I-V* relationship is linear through the origin with a slope of 23 pS (Rosenberg et al., 1986). The similarity of the conductances measured with symmetric and asymmetric Ba^{2+} concentrations, together with the clear observation of a symmetrical *I-V* relationship in symmetrical Ba^{2+} concentrations, means that the similarity of the conductances in symmetric and asymmetric Ca^{2+} concentrations suggest that a symmetrical *I-V* relationship would also be attained in symmetrical Ca^{2+} concentrations. However, the direct observation of inward currents with symmetrical Ca^{2+} and full support for the conclusion of pore symmetry with respect to Ca^{2+} permeation awaits techniques that allow tail current measurements after repolarization in symmetrical Ca^{2+} solutions.

Block of Ba^{2+} Currents by Internal Cadmium

The observation that the net rate of efflux of Na^+, Ba^{2+}, and Ca^{2+} through L-type Ca channels was identical to the net rate of influx suggested that the binding site(s) to which the ions bound as they traversed the pore were functionally symmetrical within the channel. That is, the results suggested that there was an ion-binding site accessible from the internal solution that was functionally identical to a site accessible from the external solution. An alternative way to test the functional symmetry of the ion permeation pathway is to study the effect of ionic channel blockers from each side of the channel. It is well established that L-type Ca channels are blocked by low concentrations of Cd^{2+} in the external solution (e.g., Lansman et al., 1986). In planar lipid bilayers the K_d for external Cd^{2+} block was estimated to be 36 μM (Rosenberg et al., 1988), in agreement with experiments with cell-attached patches of heart cells (Lansman et al., 1986). However, previous reports (Huang, Quayle, Worley, Standen, and Nelson, 1989) indicated that internal applications of 10 mM Cd^{2+} had no effect on the conductance of single L-type Ca channels from smooth muscle cells. Thus, we performed a test to see if Cd^{2+} blocked cardiac L-type Ca channels with high affinity from the internal solution.

Fig. 3 shows that low concentrations of Cd^{2+} in the intracellular solution also blocked inward Ba^{2+} currents through L-type Ca channels. This block was seen as a concentration-dependent reduction in the inward current amplitude (Fig. 3 *A*). The concentration dependence of the block was quantified by plotting the unitary current amplitude as a function of the Cd^{2+} concentration (Fig. 3 *B*). Superimposed on the data is the curve that describes a one-to-one blocking interaction:

$$i = i_{(Cd=0)} * \{1/(1 + [Cd]/K_{d,app})\} \quad (1)$$

The value of $K_{d,app}$ was 31.5 μM, and values of 30–40 μM were obtained in five other experiments. These values are in good agreement with those found for Cd^{2+} block

from the extracellular side, suggesting that the affinity of the Cd^{2+}-binding site accessed from the inside is similar to that accessed from the outside.

There was a subtle difference in the nature of Cd^{2+}-block from the two sides of the channel. Previous results with similar recording conditions and identical bandwidth limitations showed that externally applied Cd^{2+} produced a "flickery" block with a clear increase in the noise of the open, partially blocked channel (Rosenberg et al., 1988). In contrast, the data in Fig. 3 show little evidence of an increase in the noise level of the open-channel currents recorded in the presence of internal Cd^{2+},

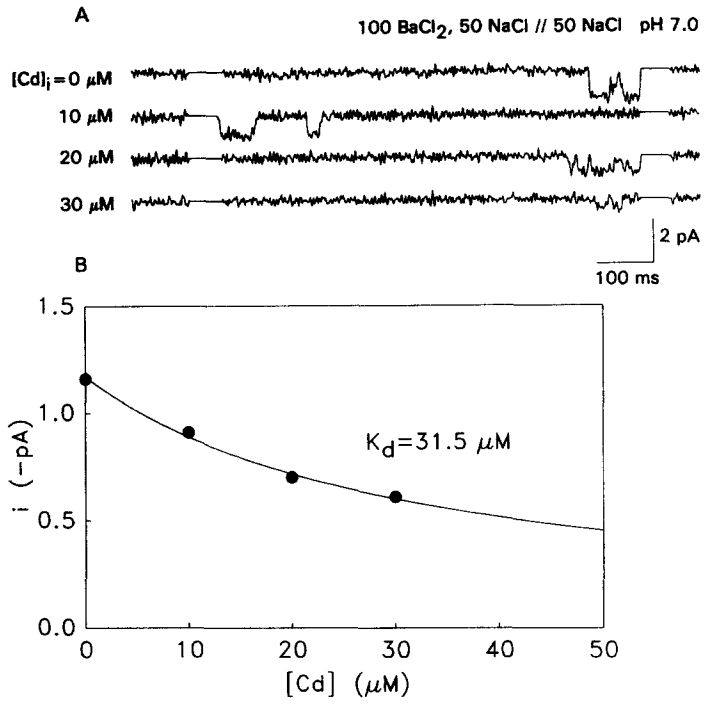

FIGURE 3. Block of inward Ba^{2+} currents by internal cadmium. HP = −70 mV, TP = 0 mV. External solution contained 100 mM $BaCl_2$; both solutions contained 50 mM NaCl and 10 mM HEPES-NaOH (pH 7.0). (*A*) $CdCl_2$ was added to the *trans* chamber to the final concentrations shown. Current amplitudes were measured by eye as in Fig. 1, and were plotted (*B*) vs. the concentration of Cd^{2+} in the internal solution. The curve represents the nonlinear least-squares fit to Eq. 1, with a K_d of 31.5 μM.

suggesting that under these conditions the blocking and unblocking transitions are too fast to be resolved. This suggests that the blocking and unblocking rates from the inside are significantly faster than those from the outside. The difference in the on-rates can be accounted for by competition for a single site: when Cd^{2+} enters the pore from the outside, it competes with Ba^{2+} for access to an intrapore site, so its on-rate is slower than when it enters the pore from the inside where there are no other divalent ions. The difference in off-rates could be due to ion–ion interactions within the pore: the exit from an internal site would be speeded up by the occupancy

of an outer site by Ba^{2+}, whereas the exit from the external site is unaffected by the concentration of Ba^{2+} in the external solution (Lansman et al., 1986). This qualitative analysis of the kinetics of Cd^{2+} block from the inside and the outside suggests that Cd^{2+} binds to an intrapore binding site near the external end of the pore when it gains access from the external solution, that it binds to a different intrapore binding site in contact with the internal solution when it gains access from the internal solution, and that at 0 mV there is very little movement of Cd^{2+} within the pore.

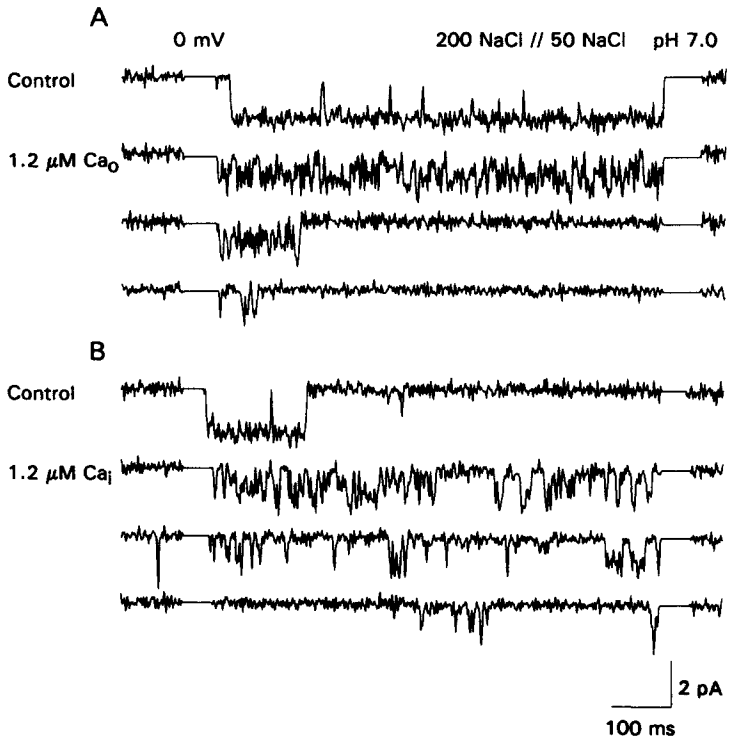

FIGURE 4. Block of inward Na^+ currents at 0 mV by external (*A*) and internal (*B*) 1.2 μM Ca^{2+}. External solution contained 200 mM NaCl, internal solution contained 50 mM NaCl, and both solutions contained 10 mM HEPES-NaOH (pH 7.0) and 1 mM HEDTA. HP = −70 mV, TP = 0 mV. After obtaining control recordings, $CaCl_2$ (0.225 mM) was added to either the *cis* or *trans* solutions (*A* and *B*, respectively), raising free Ca^{2+} to 1.2 μM. In each panel there is one control recording and three recordings in the elevated Ca^{2+}.

Block of Inward Na^+ Currents by External and Internal Ca^{2+}

Since Ca^{2+} is the physiologically preferred ion of L-type Ca channels, it is the interaction of Ca^{2+} with ion-binding sites within the pore of the channel that is most interesting. Thus, we set out to observe the block of Na^+ currents through the channels by low concentrations of Ca^{2+} in either internal or external solutions.

Fig. 4*A* shows that the block of inward Na^+ currents by external Ca^{2+} can be partially resolved under our recording conditions. In this experiment, the concentra-

tions of Na^+ in the external and internal solutions were 200 and 50 mM, respectively, and inward currents were evoked by a depolarization to 0 mV. With 1.2 μM free Ca^{2+} in the external solution, the long channel openings were disrupted by rapid, partially resolved transitions toward the closed-channel level.

Fig. 4 *B* shows that virtually the same effect is observed when 1.2 μM Ca^{2+} was added to the internal solution; well-resolved channel openings were interrupted by rapid, poorly resolved blocking transitions. An examination of the records indicates that the overall effect of the internal Ca^{2+} was approximately the same as the external Ca^{2+}, indicating that the affinity of both sides of the channel for Ca^{2+} was approximately the same.

We wanted to determine the affinity of Ca^{2+} binding to each side of the channel, but we could not directly measure the blocked- and unblocked-time distributions because the bandwidth limitations of the planar lipid bilayer recordings were too severe to permit complete resolution of the blocking–unblocking transitions. Instead, we evaluated the blocking and unblocking rates by fitting amplitude histograms of filtered current records of open, blocked channels to the normalized beta distribution:

$$f(y) = y^{a-1}(1 - y)^{b-1} \tag{2}$$

where y is the range of amplitudes between 0 and 1, $a = \alpha\tau$, $b = \beta\tau$, α is the unblocking rate, β is the blocking rate, and τ is the effective time constant of the filter ($0.228/f_c$) (Yellen, 1984). This analysis assumes that the block arises from a filtered, two-state (blocked–unblocked) process. We also assume that the blocked state passes no current, as shown by Hess et al. (1989). The beta distribution was convolved with the Gaussian distribution of the closed-channel noise before fitting. This technique has been shown to faithfully reproduce the rates of simple blocking–unblocking transitions in several experimental situations where there was incomplete resolution due to bandwidth limitations (Yellen, 1984; Pietrobon et al., 1989).

Amplitude histograms (plotting the number of events at a given current level versus the current amplitude from the fully closed to the fully open current level) constructed from open channel events that were partially blocked by external and internal 1.2 μM Ca^{2+} are shown in Fig. 5. Superimposed on each histogram is the beta distribution that was determined by eye to provide the best overall fit. The blocking and unblocking rates (β and α, respectively) were then extracted from the beta distributions. For externally applied Ca^{2+} the blocking rate was estimated to be 930 s^{-1} and the unblocking rate was 820 s^{-1}. For internally applied Ca^{2+} the blocking and unblocking rates were 576 and 430 s^{-1}, respectively.

The K_d's for block by external and internal Ca^{2+} were determined from the equation:

$$K_d = (\alpha/\beta)\,[Ca^{2+}] \tag{3}$$

Thus, the K_d for the block by external Ca^{2+} is ~1.1 μM, and that for internal Ca^{2+} is ~0.9 μM. Other experiments with different concentrations of Ca^{2+} produced similar results (not shown).

Although the estimated blocking and unblocking rates for internal Ca^{2+} are different from those estimated for external Ca^{2+}, the calculated K_d values are very

similar. Because the number of samples used to create the amplitude histograms was rather low (limited in part by Ca channel rundown in the bilayers), the fits of the beta distributions were not precise and could vary by up to 15%. Therefore, although the confidence in the accuracy of the estimated rate constants is rather low, the similarity in the estimated K_d's supports the view that the interaction of Ca^{2+} with the pore is symmetrical; that is, the affinity of Ca^{2+} binding to the pore appears to be the same at the external and internal entrances to the pore (see Discussion).

Block of Currents in Symmetrical Na^+ by External and Internal Ca^{2+}

The fact that the affinity of Ca^{2+} interaction with the pore appears to be the same from both sides raises the question: Is Ca^{2+} binding to the same site within the pore, but approaching it from opposite directions? One way to answer this question is to determine the location within the membrane electric field of the Ca^{2+} binding sites accessed from the external and internal solutions. To do this, we recorded currents

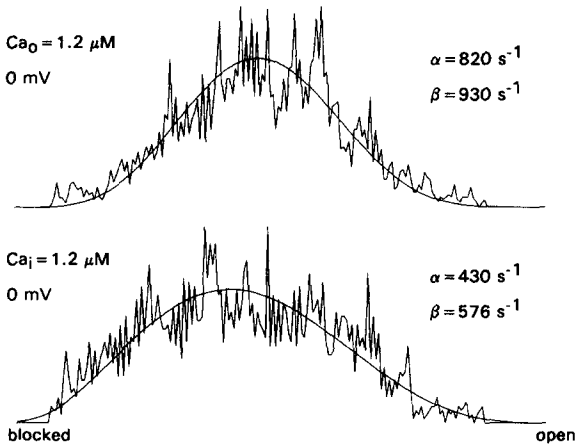

FIGURE 5. Quantitative analysis of the block of inward Na^+ currents at 0 mV by external and internal Ca^{2+}. Blocked currents were refiltered at 30 Hz, and periods with one open channel were used to form amplitude histograms. Superimposed on each histogram is the beta distribution representing a two-state, blocking–unblocking process filtered through a first-order filter. Data were fit by eye.

with symmetrical concentrations of Na^+ (as in Fig. 1) and then evaluated the concentration and voltage dependence of the block of the currents by externally and internally applied Ca^{2+}.

Fig. 6 *A* shows a control recording of outward current at +30 mV and four records of the block by 1.8 μM external Ca^{2+}. As in Fig. 4, the block is seen as partially resolved transitions toward the zero current level. Fig. 6 *B* shows the block by external Ca^{2+} of inward currents at −30 mV from the same experiment. The block was somewhat more complete at −30 mV than at +30 mV, as expected if the location of the blocking site is within the membrane, where access and egress is sensitive to the transmembrane electric field.

Fig. 7 shows the effect of 1.2 μM internal Ca^{2+} on outward currents at +30 mV (Fig. 7 *A*) and on inward currents at −30 mV (Fig. 7 *B*). The block of outward currents is much more apparent than that of inward currents, in agreement with Hess et al. (1989), again suggesting that the location of the blocking site is located within the pore, sensitive to the transmembrane electric field.

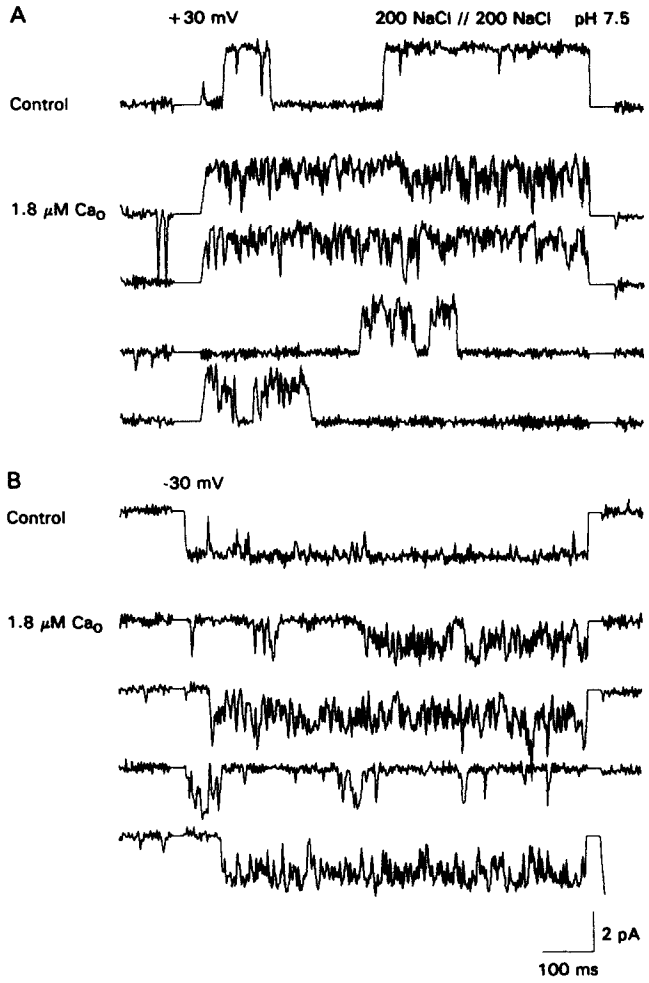

FIGURE 6. Currents in symmetrical Na^+ blocked by 1.8 μM external Ca^{2+}. Control recordings at TP = ±30 mV were obtained in symmetrical 200 mM NaCl, 10 mM HEPES-NaOH (pH 7.5), and 1 mM HEDTA. $CaCl_2$ (0.6 mM) was then added to the external solution, raising free Ca^{2+} to 1.8 μM. (*A*) Recordings showing poorly resolved rapid block of outward currents were obtained; HP = −70 mV, TP = +30 mV. (*B*) Block of inward currents at TP = −30 mV. Same experiment as shown in *A*.

Quantitative analysis of the results from experiments shown in Figs. 6 and 7 is shown in Fig. 8. These are the amplitude histograms of open, partially blocked channels at different membrane potentials with Ca^{2+} present in either the internal or external solution, and the beta distributions determined by eye to provide the best overall fit. The second and third histograms show that the K_d for block of inward current (−30 mV) by external Ca^{2+} (~2.4 μM), is approximately equal to the K_d for block of outward current (+30 mV) by internal Ca^{2+} (~2.2 μM). Similarly, the first and fourth histograms show that the K_d for block of outward current by external Ca^{2+}

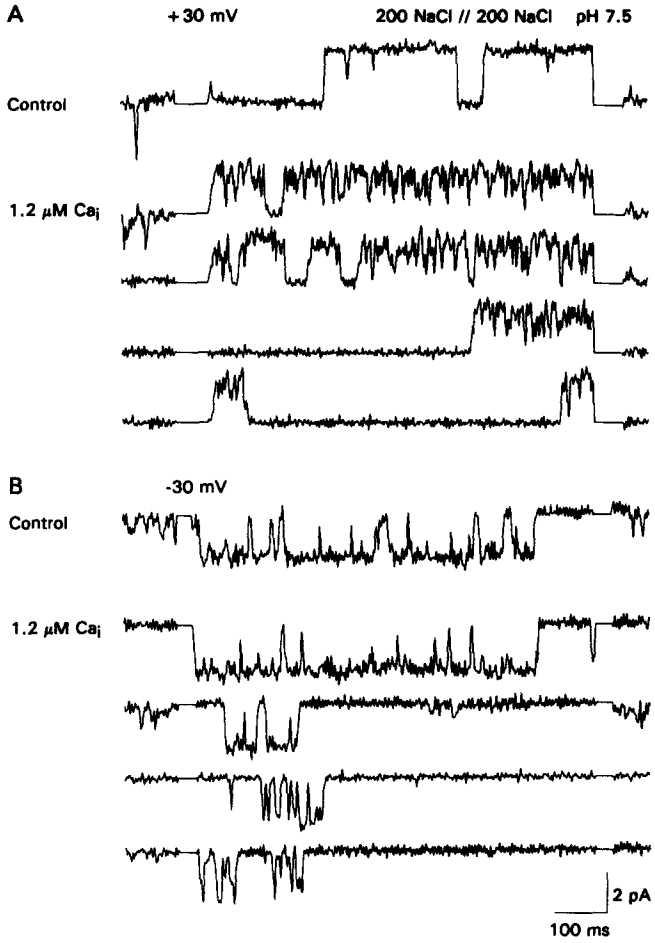

FIGURE 7. Currents in symmetrical Na^+ blocked by 1.2 μM internal Ca^{2+}. Control recordings at TP = ±30 mV were obtained in symmetrical 200 mM NaCl, 10 mM HEPES-NaOH (pH 7.5), and 1 mM HEDTA. $CaCl_2$ (0.5 mM) was then added to the internal solution, raising free Ca^{2+} to 1.2 μM. (*A*) Recordings showing poorly resolved rapid block of outward currents were obtained; HP = −70 mV, TP = +30 mV. (*B*) Block of inward currents at TP = −30 mV. Same experiment as shown in *A*.

(~4.5 μM) is very similar to the K_d for block of inward current by internal Ca^{2+} (~4.6 μM).

Voltage Dependence of Block

To complete the analysis, Fig. 9 shows a semilogarithmic plot of the calculated K_d's for block by external and internal Ca^{2+} from several experiments as a function of the test potential. This plot shows that increasingly depolarized test potentials increase the K_d (i.e., decrease the affinity of binding) for external Ca^{2+}, but lower the K_d (increase the affinity) for block by internal Ca^{2+}.

The slope of the plot provides a measure of the fractional electrical distance "sensed" by an ion as it enters and exits a binding site within the field, according to the equation:

$$\ln K_d(V) = \ln K_d(0) - [d * zF/RT] * V \quad (4)$$

where d is the fractional electrical distance, V is the transmembrane voltage, R, T, and F have their usual meanings, and z, the valence of the blocking ion, is 2 (Woodhull, 1972). The slopes of the lines in Fig. 9 suggest that d is 0.13 ± 0.07 for external Ca^{2+} and −0.17 ± 0.07 for internal Ca^{2+}. This means that the site to which external Ca^{2+}

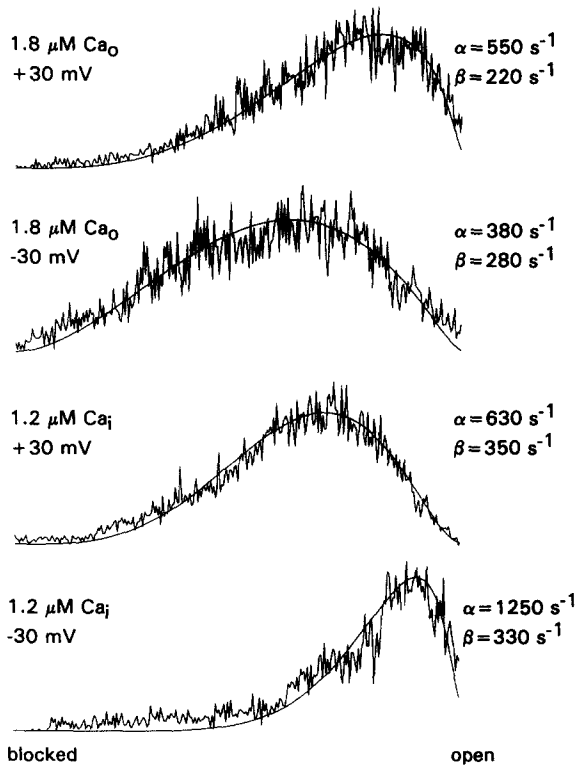

FIGURE 8. Quantitative analysis of the block of symmetrical Na^+ currents by external and internal Ca^{2+}. Amplitude histograms were constructed and fitted as described in Methods and Fig. 5 legend. K_d's, calculated from Eq. 2, are 4.5 μM for external Ca^{2+} at +30 mV, 2.4 μM for external Ca^{2+} at −30 mV, 2.2 μM for internal Ca^{2+} at +30 mV, and 4.6 μM for internal Ca^{2+} at −30 mV.

binds is ~15% of the electrical distance across the membrane from the outside of the pore, and the site to which internal Ca^{2+} binds is ~15% of the electrical distance from the inside of the pore.

If external and internal Ca^{2+} were binding to the same site within the pore, the electrical distances measured would be expected to sum to unity. The observation that the sum of the electrical distances measured for internal and external Ca^{2+} is significantly less than 1.0 is strong evidence that Ca^{2+} binds to different sites when it enters the pore from either end. This provides direct evidence for the existence of at least two high-affinity Ca^{2+}-binding sites within the pore of L-type Ca channels. Both

sites appear to have the same affinity for Ca^{2+} ($K_d \approx 2$ μM at 0 mV in the presence of 200 mM Na^+), and, within the limits of resolution, both sites appear to be located ~15% of the electric field from each end of the pore.

DISCUSSION

Evidence for Pore Symmetry of L-Type Ca Channels

Previous studies have shown that inward and outward currents through L-type Ca channels had the same magnitude when equal concentrations of Ba^{2+} (Rosenberg et al., 1988) and Na^+ (Hess et al., 1989) were present on each side of the channel. This was taken as evidence that the permeation pathway through which the ions had to pass was functionally symmetrical within the electric field of the membrane.

We provide additional evidence that strengthens this hypothesis. In addition to Ba^{2+} and Na^+, we now provide indirect evidence suggesting that the permeation of

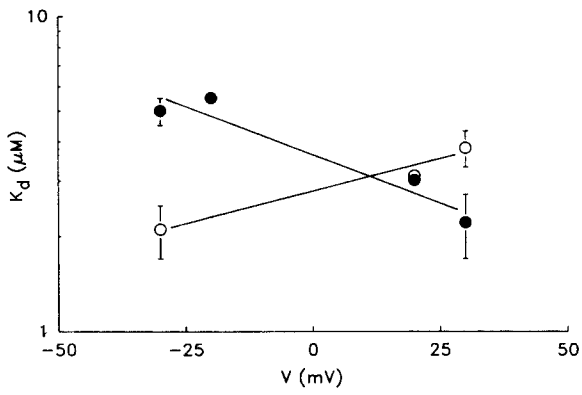

FIGURE 9. Semi-logarithmic plot of K_d vs. membrane potential. Blocking and unblocking rates for internal (●) and external Ca^{2+} (○) at different test potentials were determined as shown in Fig. 8. Data at ±30 mV represent the mean and SEM from three different experiments. Lines represent the linear least-squares fit of the data. Since $K_d(V) = K_d(0)$ exp $(-dzVF/RT)$, the slopes of the lines give d, the fractional electrical distance from the bulk solution to the Ca^{2+} binding site. From the outside, $d = 0.13 \pm 0.07$. From the inside, $d = 0.17 \pm 0.07$.

Ca^{2+} is symmetrical. Furthermore, quantitative analysis of the binding interaction of Ca^{2+} with the pore, measured as a rapid, poorly resolved blockade of Na^+ currents, indicates that Ca^{2+} binds to two sites within the pore. Although resolution is limited, each site appears to be located ~15% of the electric field into the pore from each end. Each of these sites has a high affinity for Ca^{2+} ($K_d \approx 2$ μM).

We have observed that internal Cd^{2+} blocks the channels with approximately the same affinity as external Cd^{2+}. These results are in conflict with the observations of Huang et al. (1989), suggesting possible differences between L-type Ca channels from smooth muscle cells and cardiac sarcolemma with respect to Cd^{2+} blockade.

Comparison of Blocking and Unblocking Rates with Previous Results

As stated above, our confidence in the accuracy of the absolute blocking and unblocking rates is low, primarily because the "noise" of the amplitude histograms created by a relatively small data set do not permit a precise fit to the beta

distribution. For comparison, our blocking rate of 930 s^{-1} (for block by 1.2 μM external Ca^{2+} at 0 mV; Fig. 5) translates into a value of 7.8×10^8 $M^{-1}s^{-1}$, and a blocking rate of 280 s^{-1} (for block by 1.8 mM external Ca^{2+} at −30 mV; Fig. 8) corresponds to 1.6×10^8 $M^{-1}s^{-1}$, compared with the value of 4.8×10^8 $M^{-1}s^{-1}$ obtained from data of fully resolved block of Li^+ currents by Ca^{2+} (Lansman et al., 1986). Thus, our blocking rates are scattered substantially around the rate determined directly (Lansman et al., 1986).

However, because the blocking and unblocking rates are extracted simultaneously from a single fit of the histogram data, and because the K_d's are calculated by the division of α/β, systematic errors in the absolute rates due to "noisy" histograms tend to cancel. Thus, the systematic errors in the K_d values extracted from the histograms are substantially less than the errors in the absolute rates. This is supported by the fairly small error bars in Fig. 9.

Lansman et al. (1986) showed that the unblocking rate for externally applied Ca^{2+} increased as the voltage was made more negative over the voltage range between −60 and −20 mV, as expected if Ca^{2+} can exit by being driven through the pore into the cell. Our results, however, indicate that the unblocking rate for externally applied Ca^{2+} decreased when the voltage was changed from +30 mV to −30 mV. The difference is attributable to the different voltage ranges in the two experiments; in our experiments permeation of the Ca^{2+} ions was relatively rare compared with exit of the bound Ca^{2+} back to the external solution. Similarly, Fukushima and Hagiwara (1985) showed that the extent of Ca^{2+}-block of Na^+ currents through Ca channels in whole cells was biphasic, with a maximum at around −20 mV. Polarization of the cell below −20 mV decreased the extent of block, presumably because Ca^{2+} was passing into the cell as seen by Lansman et al. (1986), and depolarization above −20 mV decreased the extent of block, presumably because Ca^{2+} was exiting back into the external solution, as seen in this report.

Implications for Models of the Pore of Ca Channels

Our results provide direct evidence for two intrapore binding sites for Ca^{2+}, as suggested by previous experiments and quantitative modeling (Almers and McCleskey, 1984; Hess and Tsien, 1984; Campbell, Rasmussen, and Strauss, 1988*c*). Are our results in conflict with the three-site model proposed by Yue and Marban (1990)? The answer is no, because the fractional electrical distances we have measured for each of the two binding sites is only 15%, leaving 70% of the electrical distance across the membrane unaccounted for. Do our data actually support the three-site model? Again, the answer is no; our data support the presence of at least two ion-binding sites within the pore, but provide no information on the existence or characteristics of a proposed third site.

The model proposed by Yue and Marban (1990) is not symmetrical within the electric field, presumably to account for asymmetries in *I-V* relations when Ba^{2+} is present in the external solution only. Asymmetrical models are also suggested by the results of Fukushima and Hagiwara (1985). Our data support symmetrical models (Almers and McCleskey, 1984; Hess and Tsien, 1984; Campbell et al., 1988*c*), with the ion-binding sites located at 15, 50, and 85% of the electrical distance (for a three-site model) or at 15 and 85% (for a two site model).

Given the thickness of a cell membrane (5 nm), and some inferences about the physical separation of Ca^{2+}-binding sites in other Ca^{2+}-binding proteins, we can contemplate the implications of the electrical distances between Ca^{2+}-binding sites for the physical structure of the pore. Almers and McCleskey (1984) suggest that the distance between two intrapore binding sites could be ~ 1.15 nm, based on the crystal structure of troponin C (Kretsinger and Barry, 1975). Thus, in the two-site model, 70% of the transmembrane electrical field would fall over a distance of 1.15 nm, suggesting that 100% of the field could fall over 1.64 nm. This would leave as much as 3.36 nm of membrane thickness for wide vestibules over which the electrical field would not be expected to drop significantly. Wide, deep vestibules and short, narrow domains where ion channel selectivity mechanisms are concentrated is a common motif in channel modeling (e.g., Yellen, 1984; Dani, 1986) supported by structural data from the nicotinic acetylcholine receptor (Toyoshima and Unwin, 1988).

We thank Patricia A. Koplas, Joan E. East, and Robert M. Brosh for assistance in the preparation of cardiac sarcolemma, Drs. D. Römer, E. Rissi, and R. P. Hof, Cardiovascular Unit of Preclinical Research, Sandoz AG, Basel, Switzerland, for the gift of (+)-202-791, Ms. Jackie Hicks and Garrard Sausage Co. for providing porcine hearts, and Dr. B. Pallotta and Dr. R. Dingledine for helpful discussions and generous loans of equipment.

This work was supported by the National Institutes of Health (NS-26660) and a Grant-in-Aid from the American Heart Association. R. L. Rosenberg is an Established Investigator of the American Heart Association.

Original version received 20 July 1990 and accepted version received 14 January 1991.

REFERENCES

Almers, W., and E. W. McCleskey. 1984. Non-selective conductance in calcium channels of frog muscle: calcium selectivity in a single-file pore. *Journal of Physiology.* 353:585–608.

Almers, W., E. W. McCleskey, and P. T. Palade. 1984. A non-selective cation conductance in frog muscle membrane blocked by micromolar external calcium ions. *Journal of Physiology.* 353:565–583.

Byerly, L., P. B. Chase, and J. R. Stimers. 1985. Permeation and interaction of divalent cations in calcium channels of snail neurons. *Journal of General Physiology.* 85:491–518.

Campbell, D. L., W. R. Giles, J. R. Hume, D. Noble, and E. F. Shibata. 1988*a*. Reversal potential of the calcium current in bull-frog atrial myocytes. *Journal of Physiology.* 403:267–286.

Campbell, D. L., W. R. Giles, J. R. Hume, and E. F. Shibata. 1988*b*. Inactivation of calcium current in bull-frog atrial myocytes. *Journal of Physiology.* 403:287–315.

Campbell, D. L., R. L. Rasmussen, and H. C. Strauss. 1988*c*. Theoretical study of the voltage and concentration dependence of the anomalous mole fraction effect in single calcium channels. *Biophysical Journal.* 54:945–954.

Cohen, F. S. 1986. Fusion of liposomes to planar lipid bilayers. *In* Ion Channel Reconstitution. C. Miller, editor. Plenum Publishing Corp., New York. 131–139.

Colquhoun, D., and F. J. Sigworth. 1983. Fitting and statistical analysis of single-channel records. *In* Single-Channel Recording. B. Sakmann and E. Neher, editors. Plenum Publishing Corp., New York. 191–263.

Coronado, R., and H. Affolter. 1986. Insulation of the conductance pathway of skeletal muscle transverse tubules from the surface charge of bilayer phospholipid. *Journal of General Physiology.* 87:933–953.

Dani, J. 1986. Ion channel entrances influence permeation. *Biophysical Journal.* 49:607–618.

Ehrlich, B. E., C. R. Schen, M. L. Garcia, and G. J. Kaczorowski. 1986. Incorporation of calcium channels from cardiac sarcolemmal membrane vesicles into planar lipid bilayers. *Proceedings of the National Academy of Sciences, USA.* 83:193–197.

Friel, D. D., and R. W. Tsien. 1989. Voltage-gated calcium channels: direct observation of the anomalous mole fraction effect at the single channel level. *Proceedings of the National Academy of Sciences, USA.* 86:5207–5211.

Fukushima, Y., and S. Hagiwara. 1985. Currents carried by monovalent cations through calcium channels in mouse neoplastic B lymphocytes. *Journal of Physiology.* 358:255–284.

Hadley, R. W., and J. Hume. 1987. An intrinsic potential-dependent inactivation mechanism associated with calcium channels in guinea pig myocytes. *Journal of Physiology.* 389:205–222.

Hess, P., J. B. Lansman, and R. W. Tsien. 1986. Calcium channel selectivity for divalent and monovalent cations. *Journal of General Physiology.* 88:293–319.

Hess, P., B. Prod'hom, and D. Pietrobon. 1989. Mechanisms of interaction of permeant ions and protons with dihydropyridine-sensitive calcium channels. *Annals of the New York Academy of Sciences.* 560:80–93.

Hess, P., and R. W. Tsien. 1984. Mechanism of ion permeation through calcium channels. *Nature.* 309:453–456.

Huang, Y., J. M. Quayle, J. F. Worley, N. B. Standen, and M. T. Nelson. 1989. External cadmium and internal calcium block of single calcium channels in smooth muscle cells from rabbit mesenteric artery. *Biophysical Journal.* 56:1023–1028.

Kostyuk, P. G., and S. L. Mironov. 1986. Some predictions concerning the calcium channel model with different conformational states. *General Physiology and Biophysics.* 5:649–654.

Kostyuk, P. G., S. L. Mironov, and M. Shuba. 1983. Two ion-selecting filters in the calcium channel of the somatic membrane of mollusc neurons. *Journal of Membrane Biology.* 76:83–93.

Kretsinger, R. H., and C. D. Barry. 1975. The predicted structure of the calcium-binding component of troponin. *Biochimica et Biophysica Acta.* 405:40–52.

Lansman, J. B. 1990. Blockade of current through single calcium channels by trivalent lanthanide cations. *Journal of General Physiology.* 95:679–696.

Lansman, J. B., P. Hess, and R. W. Tsien. 1986. Blockade of current through single calcium channels by Cd^{2+}, Mg^{2+}, and Ca^{2+}. *Journal of General Physiology.* 88:321–347.

Lee, K. S., and R. W. Tsien. 1984. High selectivity of calcium channels in single ventricular heart cells of the guinea pig. *Journal of Physiology.* 354:253–272.

Ma, J., and R. Coronado. 1987. Calcium channel conductance-activity curve in symmetrical barium solutions reveals multiple binding sites. *Biophysical Journal.* 51:423*a*. (Abstr.)

Martell, A. E., and R. M. Smith. 1974. Critical Stability Constants. Vol. 1: Amino Acids. Plenum Publishing Corp., New York. 199–202.

McDonald, T. F., A. Cavalie, W. Trautwein, and D. Pelzer. 1986. Voltage-dependent properties of macroscopic and elementary calcium channel currents in guinea pig ventricular myocytes. *Pflügers Archiv.* 406:437–448.

Pietrobon, D., and P. Hess. 1988. Conformational changes associated with ion permeation in L-type calcium channels. *Nature.* 333:373–376.

Pietrobon, D., B. Prod'hom, and P. Hess. 1989. Interactions of protons with single open L-type calcium channels. *Journal of General Physiology.* 94:1–21.

Rosenberg, R. L., X.-h. Chen, and P. A. Koplas. 1990. Functional symmetry of L-type calcium channels. *Biophysical Journal.* 57:425*a*. (Abstr.)

Rosenberg, R. L., P. Hess, J. P. Reeves, H. Smilowitz, and R. W. Tsien. 1986. Calcium channels in planar lipid bilayers: insights into mechanisms of ion permeation and gating. *Science.* 231:1564–1566.

Rosenberg, R. L., P. Hess, and R. W. Tsien. 1988. Cardiac calcium channel in planar lipid bilayers. *Journal of General Physiology.* 92:27–54.

Toyoshima, C., and N. Unwin. 1988. Ion channel of acetylcholine receptor reconstructed from images of postsynaptic membranes. *Nature.* 336:247–250.

Tsien, R. W., P. Hess, E. W. McCleskey, and R. L. Rosenberg. 1987. Calcium channels: mechanisms of selectivity, permeation, and block. *Annual Review of Biophysics and Biophysical Chemistry.* 16:265–290.

Woodhull, A. 1972. Ionic blockade of sodium channels in nerve. *Journal of General Physiology.* 61:687–708.

Yellen, G. 1984. Ionic permeation and blockage in Ca^{2+}-activated K^+ channels of bovine chromaffin cells. *Journal of General Physiology.* 84:157–186.

Yue, D. T., and E. Marban. 1990. Permeation in the dihydropyridine-sensitive calcium channel. *Journal of General Physiology.* 95:911–939.